

Molecular Dynamics of Poiseuille Flow and Moving Contact Lines

Joel Koplik, Jayanth R. Banavar, and Jorge F. Willemsen

Schlumberger-Doll Research, Ridgefield, Connecticut 06877

(Received 21 October 1987)

We report on molecular-dynamics simulations of the low-Reynolds-number flow of Lennard-Jones fluids through a channel. Application of a pressure gradient to a single fluid produces Poiseuille flow with a no-slip boundary condition and Taylor-Aris hydrodynamic dispersion. For an immiscible two-fluid system we find a (predictable) static contact angle and, when accelerated, velocity-dependent advancing- and receding-contact angles. The approximate local velocity field is obtained, in which the no-slip condition appears to break down near the contact line.

PACS numbers: 47.15.Gf, 51.10.+y, 61.20.Ja

Although the low-Reynolds-number flow of continuum Newtonian fluids has been successfully described by the Stokes equations for over a century, there remain a number of unsettled questions concerning the appropriate boundary conditions at solid surfaces and fluid interfaces. For example, overwhelming phenomenological evidence supports the "no-slip" condition of zero fluid velocity at a solid boundary,¹ yet there is no compelling theoretical argument for why this should be the case.² A problem of principle arises when a meniscus separating two immiscible fluids moves along a solid surface. When the Stokes equations are combined with the usual boundary conditions, the viscous dissipation diverges logarithmically at the contact line.³ This singularity indicates that the problem is not properly formulated, but at present the cure is not known. Various proposals have been advanced^{4,5} to yield a finite result, e.g., a finite "slip length," an appeal to surface roughness, nontrivial interfacial shapes near the solid, and precursor films, but no consensus exists.

In these and related problems, the macroscopic flow description must be augmented with knowledge of the microscopic physics of the boundary region between the fluids. To this end, we have carried out molecular dynamics (MD) simulations^{6,7} of viscous fluid flows past solid boundaries. We have studied systems consisting of 1536 molecules (per fluid) confined to a region of size 40–100 Å, over times up to 10⁻⁹ sec, the computations requiring hours of central processing unit time on a Cray XMP-12. Our results indicate that even such a small system behaves in almost all respects like a continuum fluid in motion.

The starting point is a standard molecular-dynamics code⁸ in which each pair of molecules interacts through a Lennard-Jones potential

$$V_{LJ}(r) = 4\epsilon \left[\left(\frac{r}{\sigma} \right)^{-12} - \left(\frac{r}{\sigma} \right)^{-6} \right] + r\delta V \quad (1)$$

cut off at $r = 2.5\sigma$, where δV is chosen so that the force vanishes at the cutoff. For numerical illustration, we will

refer to parameters appropriate for liquid argon, where the distance and energy scales are $\sigma = 3.4$ Å and $\epsilon/k_B = 120$ K, the natural time unit is $\tau = \sigma(m/\epsilon)^{1/2} = 2.16 \times 10^{-12}$ sec, and the molecular mass is $m = 40$ a.u. Newton's law is numerically integrated with a fifth-order predictor-corrector scheme, with a time step of 0.005τ . The molecules are initialized on an fcc lattice whose spacing is chosen to obtain the desired density, with initial velocities randomly assigned subject to a fixed temperature. The substance is then allowed to melt. The system at rest is placed in a box with periodic boundary conditions on all sides, so that a molecule exiting from the box is reinserted on the opposite face, and periodic copies of the molecules are used in the force computation. We chose density $\rho = 0.8$ and temperature $1.2\epsilon/k_B$.

We have modified this algorithm to provide constraining walls on two sides, while retaining periodicity in the other two directions. In contrast to most earlier work with solid boundaries,⁹⁻¹² we create a wall with a molecular structure.¹³ To this end, we assign the top and bottom two layers of the initial fcc lattice a heavy mass, $m_H = 10^{10}m$, but allow these to move in accord with the equations of motion. In this way collisions between fluid and wall molecules conserve energy, and the walls retain their integrity over the duration of the simulation, although eventually they would disintegrate. In Fig. 1 we show an x - z snapshot of instantaneous molecule positions after 4000 time steps of constant-temperature equilibration, in which molecules at all values of y are superposed. Near the walls one sees molecular ordering both spanwise in z , consistent with other molecular-dynamics studies of fluid systems with boundaries,^{11,12} and along the wall as in experiment.¹⁴

We simulate Poiseuille flow by introducing an analog of gravity—a force $mg\hat{x}$ applied to each particle. The key problem here is to obtain a mean particle velocity as a function of z that can be distinguished from the thermal fluctuations. After trial and error we settled on values $g \sim 0.1\sigma/\tau^2$, which correspond to Reynolds numbers $\sim 0.1-1$. We compute the average velocity by binning particles in z , and finding the mean velocity in each

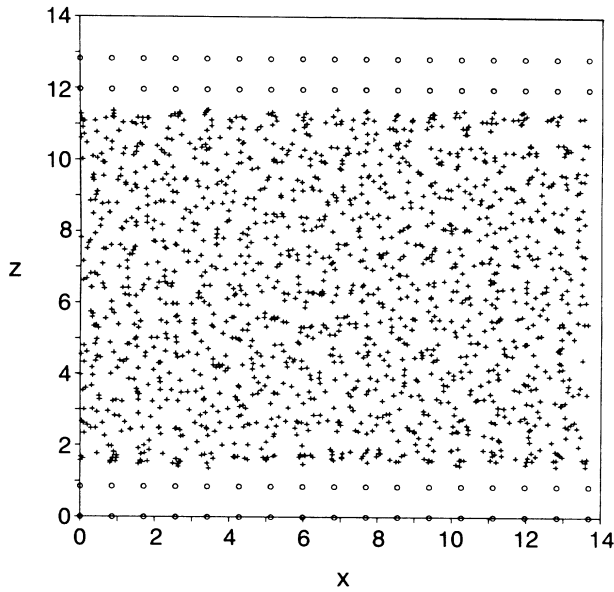


FIG. 1. Molecular configuration without flow: snapshot of particle positions after 4000 time steps.

bin averaged over 5000 time steps. We further average over initial sets of particle velocities. This procedure corresponds to a combined spatial, temporal, and run average, as would be the case in a laboratory measurement. Two alternative procedures were followed with regard to temperature, continued equilibration, or free heating (work is done on the system by gravity) in which case the temperature can rise up to 10% in our runs. Figure 2 shows a typical velocity profile; the two sets of points represent distinct realizations. The solid line is a least-squares fit to the velocity profile predicted by the Stokes equations $u(z) = (z - z_1)(z_2 - z)\rho g / 2\mu$, where $z_{1,2}$ are

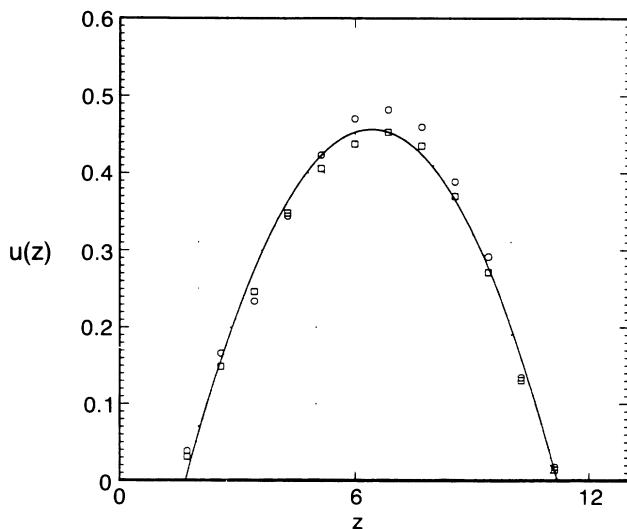


FIG. 2. Velocity profile in Poiseuille flow.

TABLE I. Measured viscosity and longitudinal dispersivity for various accelerations.

$g\tau^2/\sigma$	$\mu\sigma\tau/m$	$D_{\parallel}\tau/\sigma^2$
0	...	7.47×10^{-2}
0.025	1.85 ± 0.5	0.13
0.05	2.05 ± 0.5	0.29 ± 0.03
0.075	1.98 ± 0.5	0.58
0.1	1.85 ± 0.25	0.77 ± 0.15
0.2	1.80 ± 0.15	...
0.4	1.80 ± 0.15	...

the wall coordinates and μ the viscosity. The fit determines the viscosity with the result shown in Table I, $\mu \approx 1.9(m\epsilon)^{1/2}/\sigma^2 = 0.18$ cP for argon, consistent with values obtained by Hoover *et al.*¹⁵ The viscosity value is quite robust, showing no significant variation either as a function of MD sample size or of temperature. For all cases considered we find $z_1/\sigma = 1.57 \pm 0.3$ and $z_2/\sigma = 11.36 \pm 0.3$, with a tendency for z_1 to decrease and z_2 to increase with g . The wall layers are located at $z/\sigma = 0, 0.86, 11.97,$ and 12.83 , and the interaction potential has a hard-core radius $O(\sigma)$, so that up to an unavoidable ambiguity of $O(\sigma)$, the velocity vanishes at the "walls." Thus the no-slip condition arises *naturally* from reasonable microscopic physics assumptions.

Further insight into Poiseuille flow follows from examination of the motion of individual molecules. In Fig. 3 we show two typical trajectories, for molecules that begin near the wall and in the bulk, respectively. The motion is "Brownian," with a drift along \hat{x} , and with oc-

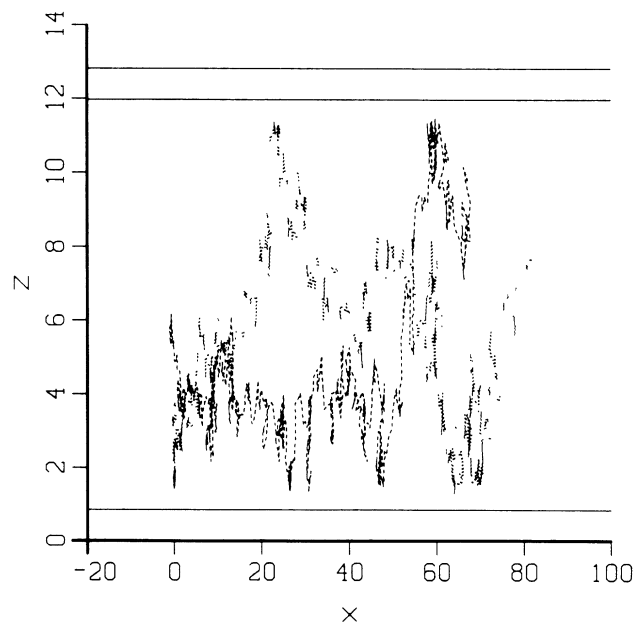


FIG. 3. Two representative particle trajectories in Poiseuille flow (dashed and dotted lines); the horizontal solid lines are the centers of the wall molecules.

casional brief localization near the wall.¹⁶ At least for the interactions used here, there is no binding to the wall.

The effect of the mean flow on diffusion can be studied quantitatively. Consider the diffusivity in the flow direction,

$$D_{\parallel} \equiv \lim_{\Delta t \rightarrow \infty} \frac{\langle (\Delta x - \langle \Delta x \rangle)^2 \rangle}{2\Delta t} = D_0 + \frac{U^2 w^2}{100D_0}. \quad (2)$$

In the first part of this equation, Δx is the displacement of a molecule in time Δt , and the brackets represent an ensemble average. The second equality is a fit to the numerical results given in Table I, where U is the average velocity, w is the width of the channel, and D_0 is the dispersivity at $g=0$. This equation should be compared with the Taylor-Aris hydrodynamic dispersivity¹⁷ for Poiseuille flow in a tube of radius r : $D_{\parallel} = D_{\text{mol}} + U^2 r^2 / 48D_{\text{mol}}$. Here we have a slot rather than a cylinder, and there is a finite-sample variation in D_0 , so that the precise numerical factor 48 need not apply, but the functional form found in the simulations agrees with the continuum result.

Having established that our methods for introducing solid walls and pressure gradients give results fully consistent with continuum fluid behavior, we introduce a mechanism for segregating immiscible fluids. A simple effective choice is to add an additional repulsive interaction between species,

$$V_{ij}(r) = V_{LJ}(r) + (c_i - c_j)^2 4\epsilon(r/\sigma)^{-6}, \quad (3)$$

where c_i is a "pseudocharge" associated with species i . The bulk interaction of pure fluid is thus unchanged, but we can vary the interaction between the two fluids A and B and with the wall W . We have chosen $c_A = +0.5$, $c_B = -0.5$, and $c_W = 0.1$. Initially 1536 molecules of each fluid occupy half an fcc lattice with a plane boundary, and the lattice then "melts" for 4000 time steps. The instantaneous configuration after 4000 steps is shown in Fig. 4(a). Outside of a thin transition zone, the fluids retain their initial segregation, and fluid A is more strongly attracted to the wall, as expected. The observed contact angle is in rough agreement with a simple argument due to Israelachvili,¹⁴ which predicts $\theta = 79^\circ$.

The last step is to apply an acceleration to each particle, with the result shown in Figs. 4(b)–4(d) at intervals of 8000 time steps after melting, for the choice $g=0.1$. Two slugs of fluids A and B chase each other in the periodic geometry, with advancing and receding contact angles which differ from the static angle and from each other. Just this kind of behavior is seen in experiments.⁴ The average velocity of the interface is roughly constant, $u_{\text{int}} \cong 0.2\sigma/\tau$, but the shape gradually changes at least in part because of the film of fluid A beginning to form along the walls. When the acceleration is turned off the slugs come to rest, and we have observed the wall film beginning to retract into the bulk.¹⁶

Having set up a successful computer model of a mov-

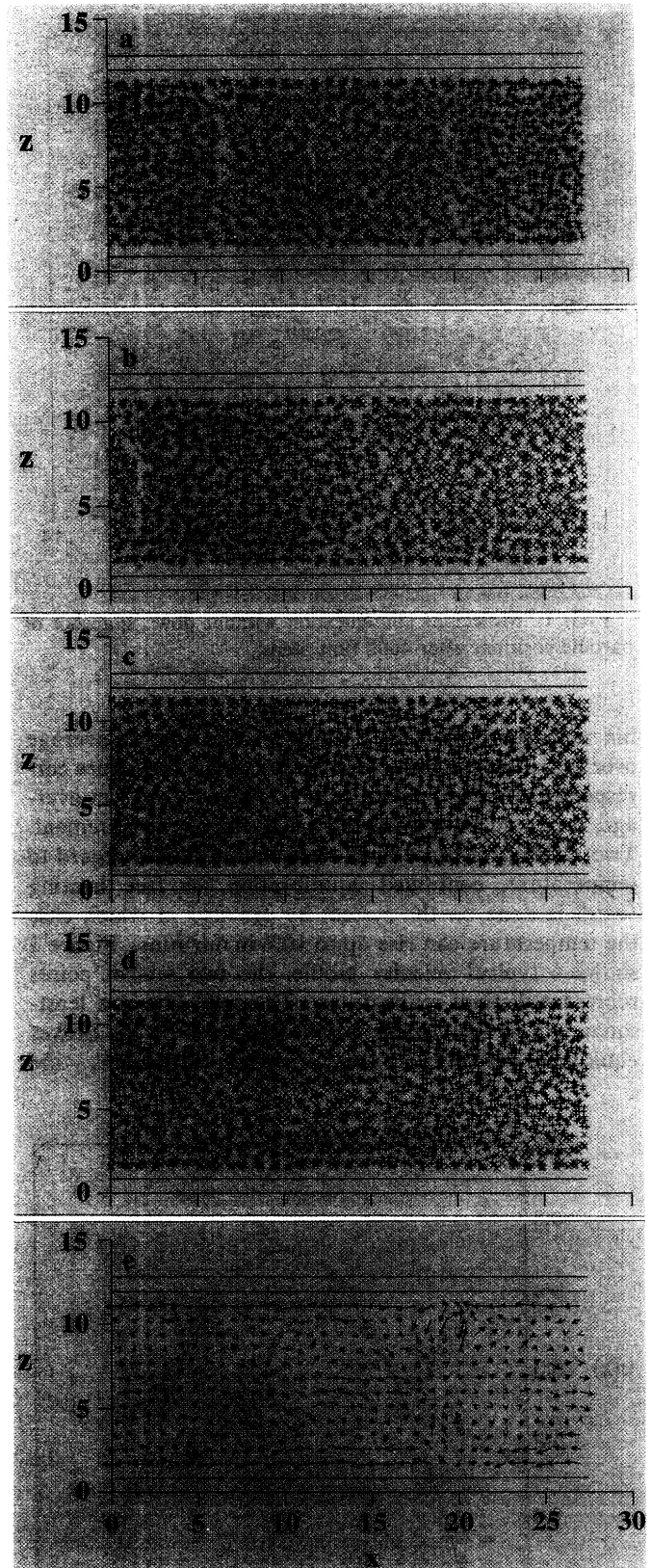


FIG. 4. Time sequence of a two-fluid system in motion: instantaneous particle positions after (a) 4000, (b) 12000, (c) 20000, and (d) 28000 time steps. (e) Average velocity field in the rest frame of the interface.

ing contact line, we can begin to ask detailed questions about the flow. Figure 4(e) shows the velocity field in the rest frame of the interface. (Note that while the interface shape changes with time, it does not do so significantly over the later time-averaging intervals, and this reference frame is sensibly defined). To obtain the figure we use a 32×16 array of x - z bins moving with the velocity of the interface, and average the velocities of molecules occupying each bin over 4000 time steps. An average bin contains eight molecules—not a large number, but enough to obtain reproducible results when different time intervals are considered. The walls are moving to the left in this reference frame, and the fluid velocity near the wall coincides with the wall velocity, *except near the contact line where the no-slip condition appears to fail*. In addition, we observe a jet of fluid into the interior from the contact line, as well as hints of closed eddies of fluid behind the interface. The presence of such jets and eddies are consistent with the experiments and kinematic analysis of Dussan and Davis.¹⁸

To summarize, we have combined several ingredients of the MD method for a novel study of viscous flows of one and two immiscible fluids near solid boundaries. Despite a computational restriction to small samples, our results in all respects display the characteristics of bulk, continuum fluid flow. This, we believe, establishes the viability of MD as a calculational method for addressing the troublesome points we discussed at the beginning. Already at this level we have illustrated the ambiguities present in the “no-slip” boundary condition, and exhibited spatial structure in the flow field for diphasic flow. We are in a position to explore many more detailed quantitative aspects of these flows, albeit somewhat slowly because of the time intensiveness of these simulations.

We thank John Ullo and Sidney Yip for launching us into MD and sharing their expertise, Elizabeth Dussan for discussions of the fluid dynamics of contact lines, and Stephen Garoff and Jaco Israelachvili for advising us

about molecular structure near solids.

¹G. K. Batchelor, *An Introduction to Fluid Dynamics* (Cambridge Univ. Press, Cambridge, 1967).

²J. C. Maxwell, *Philos. Trans. R. Soc.* **157**, 49 (1867); R. Jackson, *Transport in Porous Catalysts* (Elsevier, Amsterdam, 1977).

³C. Huh and L. E. Scriven, *J. Colloid Interface Sci.* **35**, 85 (1971).

⁴E. B. Dussan V., *Annu. Rev. Fluid Mech.* **11**, 371 (1979).

⁵P. G. De Gennes, *Rev. Mod. Phys.* **57**, 827 (1985).

⁶W. G. Hoover, *Molecular Dynamics* (Springer-Verlag, New York, 1986).

⁷*Molecular-Dynamics Simulation of Statistical Mechanics Systems*, edited by G. Ciccotti and W. G. Hoover (North-Holland, Amsterdam, 1986).

⁸J. M. Haile, *A Primer on the Computer Simulation of Atomic Fluids by Molecular Dynamics* (Clemson Univ., Clemson, SC, 1980).

⁹A. W. Lees and S. F. Edwards, *J. Phys. C* **5**, 1921 (1972).

¹⁰S. Toxvaerd, *J. Chem. Phys.* **74**, 1998 (1981).

¹¹J. J. Magda, M. Tirrell, and H. T. Davis, *J. Chem. Phys.* **83**, 1888 (1985).

¹²A. Tenenbaum, G. Ciccotti, and G. Gallico, *Phys. Rev. A* **25**, 2778 (1982); C. Trozzi and G. Ciccotti, *Phys. Rev. A* **29**, 916 (1984).

¹³G. A. Chapela, G. Saville, S. M. Thompson, and J. M. Rowlinson, *J. Chem. Soc. Faraday Trans. 2* **73**, 1133 (1977); F. F. Abraham, *J. Chem. Phys.* **68**, 3713 (1978).

¹⁴J. N. Israelachvili, *Intermolecular and Surface Forces* (Academic, London, 1985), Chap. 9.

¹⁵W. G. Hoover, D. J. Evans, R. B. Hickman, A. J. C. Ladd, W. T. Ashurst, and B. Moran, *Phys. Rev. A* **22**, 1690 (1980).

¹⁶J. Koplik, J. R. Banavar, and J. F. Willemsen, to be published.

¹⁷G. I. Taylor, *Proc. Roy. Soc. London A* **219**, 186 (1953); R. Aris, *Proc. Roy. Soc. London* **235**, 67 (1956).

¹⁸E. B. Dussan V. and S. H. Davis, *J. Fluid Mech.* **65**, 71 (1974); E. B. Dussan V., *AIChE J.* **23**, 131 (1977).

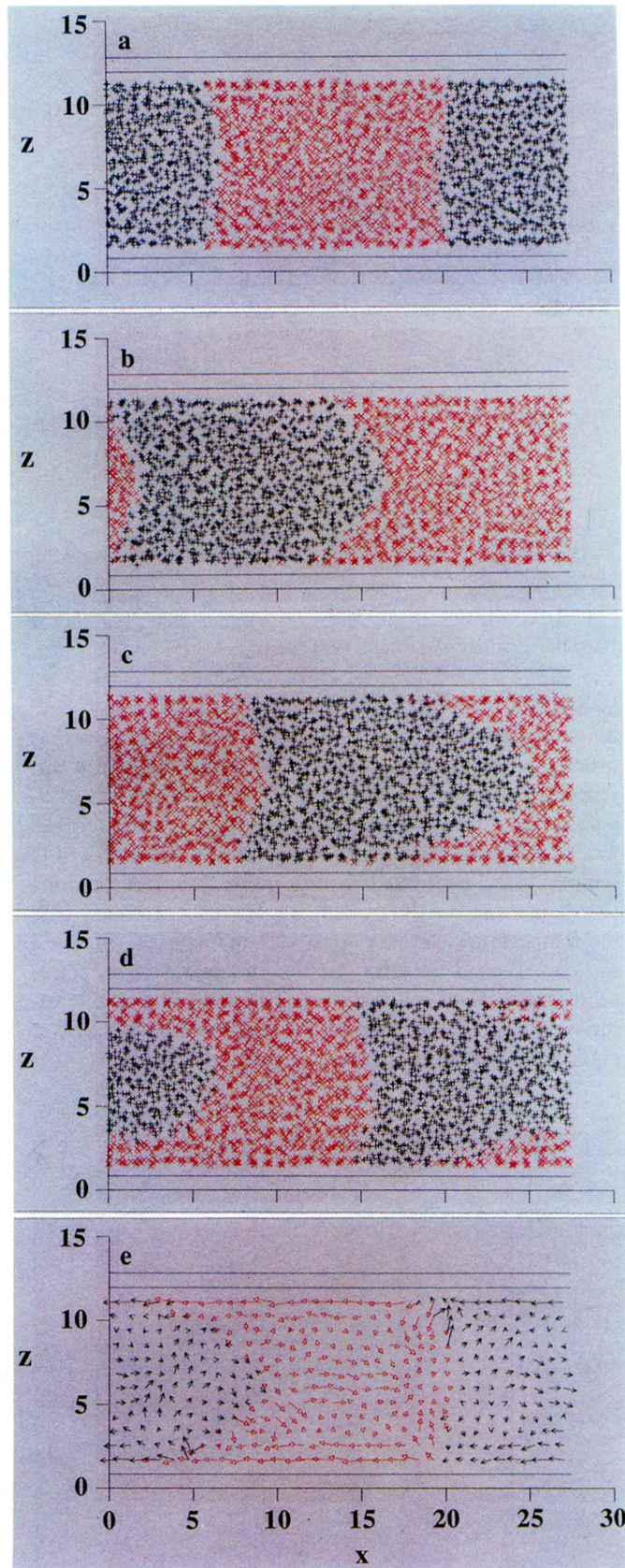


FIG. 4. Time sequence of a two-fluid system in motion: instantaneous particle positions after (a) 4000, (b) 12000, (c) 20000, and (d) 28000 time steps. (e) Average velocity field in the rest frame of the interface.